Longitudinal Scoliotic Trunk Analysis via Spectral Representation and Statistical Analysis

Ola Ahmad[1,2(✉)], Herve Lombaert[3], Stefan Parent[1,2], Hubert Labelle[1,2], Jean Dansereau[2,4], and Farida Cheriet[2,4]

[1] Université de Montréal, Montréal, Canada
olasahmad@gmail.com
[2] Centre de Recherche du CHU Sainte-Justine, Montréal, Canada
[3] INRIA, Sophia-antipolis, France
[4] École Polytechnique de Montréal, Montréal, Canada

Abstract. Scoliosis is a complex 3D deformation of the spine leading to asymmetry of the external shape of the human trunk. A clinical follow-up of this deformation is decisive for its treatment, which depends on the spinal curvature but also on the deformity's progression over time. This paper presents a new method for longitudinal analysis of scoliotic trunks based on spectral representation of shapes combined with statistical analysis. The spectrum of the surface model is used to compute the correspondence between deformable scoliotic trunks. Spectral correspondence is combined with Canonical Correlation Analysis to do point-wise feature comparison between models. This novel combination allows us to efficiently capture within-subject shape changes to assess scoliosis progression (SP). We tested our method on 23 scoliotic patients with right thoracic curvature. Quantitative comparison with spinal measurements confirms that our method is able to identify significant changes associated with SP.

1 Introduction

Scoliosis is a complex 3D deformation affecting the general appearance of torso shape. This deformation is defined by abnormal curvature of the spine accompanied by deformation of the rib cage. The standard evaluation protocols of this pathology use clinical measurements such as the Cobb Angle (CA) [7], which is based on radiographic image data and quantifies the severity of the spinal curvature. Scoliosis is more commonly diagnosed in children aged 10–18 years and may develop rapidly, to the point of requiring surgical intervention. Frequent observations are therefore required to monitor the condition during the adolescent growth spurt. An increase in CA of more than 6° indicates a worsening of the curvature [21]. But since the CA is limited to spinal curvature assessment, this measure cannot evaluate the complex deformation of the torso shape. Yet, the importance of the latter should not be underestimated as it exhibits the first symptoms of scoliosis and is the major concern for adolescent patients. Scoliosis manifests itself in shape asymmetries and a high variety of deformations of the

M. Reuter et al. (Eds.): SeSAMI 2016, LNCS 10126, pp. 79–91, 2016.
DOI: 10.1007/978-3-319-51237-2_7

Fig. 1. Sample scoliotic trunk surfaces of different patients. These examples illustrate the high variability in the shape of scoliotic trunks.

external surface of the trunk. These anomalies include deformations such as a hump at the back, a lateral shift of the trunk and asymmetries of the shoulders, scapulae, waist and hips (Fig. 1). Analysis of the scoliotic trunk shape is valuable in the clinical setting to assess the effect of surgical correction or to monitor scoliosis progression (SP), i.e. the worsening of the deformation over time. A clinical follow-up of scoliotic 3D shape deformities therefore becomes decisive for its management.

Previous approaches based on cross-sectional trunk surface analysis either describe back rotation and lateral shifts of the trunk [18,22], or quantify torso shape by three rotations in the lateral, axial and posterior-anterior planes [3]. They ignore all the local deformations of scoliotic shapes, and consequently, are limited in detecting SP. Statistical shape models [1] have been recently proposed to evaluate local shape deformations of scoliotic trunks. These models are trained on populations of normal shapes in a reduced feature space. However, the reduced space affects the statistical power of these models to reveal SP. Furthermore, these models are often biased by the control groups used to train them, and may not account for large shape variations due to normal variability across a population and to anatomical growth, as is the case in adolescents.

To overcome these issues, we propose a longitudinal analysis of scoliotic trunks based on spectral representation and statistical analysis of shapes. More specifically, a statistical shape analysis will incorporate within-subject spectral correspondence of surface models. Currently, spectral methods provide efficient tools for the representation of geometric models, e.g., meshes, shape matching [8,12,13,20], segmentation [19] and registration [15,19]. Shape spectra are isometry-invariant and are more robust to large deformations of surface models. They are considered as fingerprints of shapes [20]. Accordingly, matching shapes in the spectral domain enables accurate correspondence independently from their spatial positions in the Euclidean space. We exploit the spectral matching framework to compute correspondence between scoliotic trunk surfaces. A robust correspondence facilitates the underlying statistical analysis problem, in particular, detecting local changes between shapes. Change detection approaches in longitudinal processing provide numerous statistical tools to capture significant

differences, for instance, associated with disease progression [9] and pattern evolution [2]. Inspired by these methods, we propose the Canonical Correlation Analysis (CCA) method [11] to evaluate point-wise differences between matched shapes. Performing this analysis within subjects is useful to assess SP during clinical follow-up protocols.

We begin this paper by describing the representation of scoliotic trunks via the spectral graph. To our knowledge, this is the first time that the spectrum of the graph is used for scoliotic trunk analysis. We exploit the recent work on spectral matching [14] to find accurate correspondence maps between shape models. Spectral correspondence, together with CCA, are proposed for efficient point-wise feature comparison between longitudinally acquired scoliotic trunk shapes. We tested our method using the clinical follow-up trunk shape data of a set of patients with a specific type of scoliotic curvature: right thoracic spinal curve. Our results, when validated versus standard clinical measurements, show that significant shape changes revealed by this novel method of analysis are associated with SP.

2 Method

2.1 Spectral Representation of Trunk Surfaces

Let us assume a discrete representation of the trunk surface as a triangulated mesh. A spectral representation of the surface is then derived using the general Laplacian operator on a graph. Let $\mathcal{G} = \{\mathcal{V}, \mathcal{E}\}$ be a graph defined by the set of vertices, with spatial coordinates $\mathbf{x} = (x, y, z)^T$, and the set of edges connecting pairs of neighboring vertices. The general graph Laplacian is then formulated as $\mathcal{L} = G^{-1}(D - W)$, where W is the $|\mathcal{V}| \times |\mathcal{V}|$ weighted adjacency matrix, D is the diagonal degree matrix defined as $D_{ii} = \sum_j W_{ij}$, and G is the diagonal matrix of vertex weights, defined as $G = D$. Our weighted adjacency matrix is defined by the heat kernel $W_{ij} = \exp^{-\|\mathbf{x}_i - \mathbf{x}_j\|^2/2\sigma^2}$ ($\sigma \in \mathbb{R}$), if there is an edge connecting vertices i and j, i.e., $e_{ij} \in \mathcal{E}$; otherwise $W_{ij} = 0$. The harmonic spectrum of the shape of scoliotic trunks (see Fig. 2) is obtained from the generalized eigenvector problem $\mathcal{L} = \mathbf{U}\Lambda\mathbf{U}^{-1}$, where $\Lambda = \text{diag}(\lambda_0, \lambda_1, ..., \lambda_{|\mathcal{V}|})$ are the ordered eigenvalues and $\mathbf{U} = (U_0, U_1, ..., U_{|\mathcal{V}|})$ are their associated eigenfunctions. If the graph is connected, the first eigenvalue λ_0 is always equal to zero [4], i.e. there is no boundary condition, and the first eigenfunction U_0 is always constant. This solution is valid for trunk surfaces, since meshes are interpolated[1] to fill the holes where the trunk model is cropped off, i.e. at the arms, neck and pelvis. We leave out the first (trivial) eigenfunction corresponding to the zero eigenvalue, so that $\mathbf{U} = (U_1, ..., U_{|\mathcal{V}|})$ and λ_1 becomes the first non-zero eigenvalue of Λ. Accordingly, each mesh vertex $\mathbf{x}$ is represented in the spectral domain by the embedding $(\lambda_1^{-1/2}U_1(\mathbf{x}), ..., \lambda_K^{-1/2}U_K(\mathbf{x}))$—a row of the matrix $\mathbf{U}\Lambda^{-1/2}$.

[1] The Radial Basis Functions (RBF) algorithm [6] is used to interpolate incomplete trunk meshes and to enforce mesh connectivity.

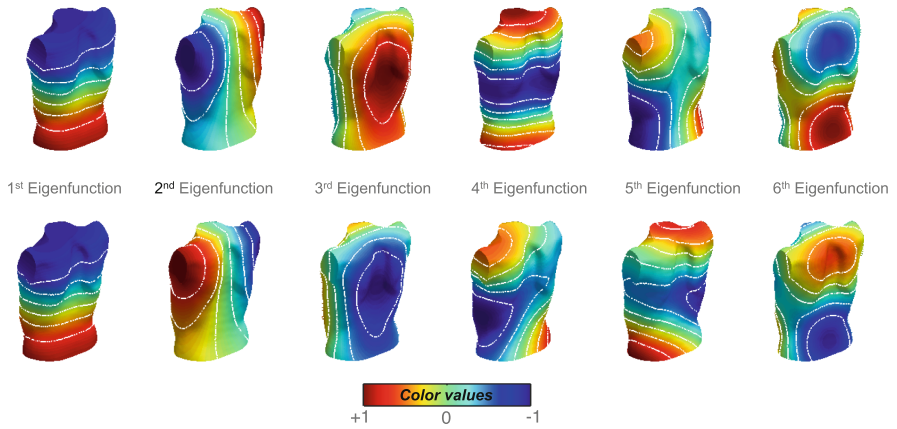

Fig. 2. Spectral representation: the first 6 eigenfunctions of the trunk shape of a patient at two different times. Eigenfunctions 2–6 are incompatible between surfaces due to sign flips and changes in the eigenfunctions. Direct matching between surfaces will thus be inconsistent. White isolines highlight the instabilities between eigenfunctions. The color scale indicates harmonic (eigenfunction) amplitude in the spectral domain. (Color figure online)

2.2 Spectral Correspondence Between Trunk Surfaces

The spectral representation defines a feature space to solve the correspondence problem between shapes via spectral matching. Spectral correspondence must however ensure stability between matched shapes [13]. Figure 2 shows incompatibility in harmonic bases 2–6 between surface models, manifested by sign flips as well as changes in the shape and orientation of the eigenfunctions, due to numerical instabilities and multiplicity ambiguities in the eigenvalues. In more recent work [14], the correspondence problem has been addressed efficiently by the transfer of harmonic weights $\Lambda^{-1/2}$ across shapes. We apply this method to find the correspondence between pairs of scoliotic trunk shapes. Let two meshes M_1 and M_2 represent the surface models of a deformable scoliotic trunk. (The term "deformable" here refers to the fact that a patient's trunk shape changes over time.) Their spectral representations can thus be defined as $\mathbf{U}_1\Lambda_1^{-1/2}$ and $\mathbf{U}_2\Lambda_2^{-1/2}$, respectively. The spectral transfer from M_1 to M_2 is defined by the $K \times K$ matrix

$$R_{12} = \left((\mathbf{U}_2)^T\mathbf{U}_2\right)^{-1}\left((\mathbf{U}_2)^T\mathbf{U}_{(1\circ c)}\right) \tag{1}$$

where c is the unknown correspondence map such that $\mathbf{U}_{(1\circ c)}\Lambda_1^{-1/2}$ is equivalent to $\mathbf{U}_2 R_{12}\Lambda_2^{-1/2}$. The correspondence c is solved as an optimization problem (detailed in [14]) that minimizes the l_2 norm of the difference

$$c = \text{argmin}_c\|\mathbf{U}_{(1\circ c)}\Lambda_1^{-1/2} - \mathbf{U}_2 R_{12}\Lambda_2^{-1/2}\|^2. \tag{2}$$

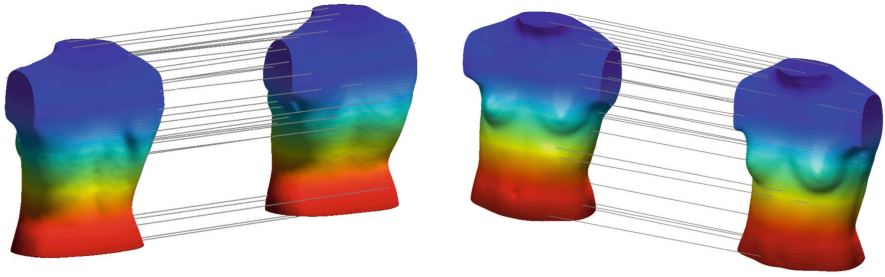

Fig. 3. Spectral correspondence resulting from the transfer of harmonic weights between two scoliotic trunks. Similar colors represent corresponding points in the posterior (left) and anterior (right) views of the trunk surfaces. Regions of the deformable shapes exhibiting local variability, e.g. the shoulders, scapulae, hips and waist, are correctly matched. (Color figure online)

Similarly, the inverse correspondence c^{-1} that maps mesh M_2 to mesh M_1 can be solved such that $\mathbf{U}_{(2 \circ c^{-1})} \Lambda_2^{-1/2}$ is equivalent to $\mathbf{U}_1 R_{21} \Lambda_1^{-1/2}$, where

$$R_{21} = \left((\mathbf{U}_1)^T \mathbf{U}_1\right)^{-1} \left((\mathbf{U}_1)^T \mathbf{U}_{(2 \circ c^{-1})}\right) \tag{3}$$

is the $K \times K$ spectral transfer matrix from M_2 to M_1. To enforce symmetry in the solution, both c and c^{-1} are used in the underlying energy function. The number of harmonic bases K determines the resolution used to compute the correspondence in the spectral domain. Since trunk shapes are smooth surfaces, it was sufficient in our experiments to compute the correspondence between their meshes using at most 20 eigenfunctions. Figure 3 gives an example of the correspondence map of a pair of trunk surfaces acquired during clinical follow-up. Corresponding points are correctly computed between the deformable shapes and are independent of local and global differences between the surface models.

2.3 Statistical Analysis of Local Deformations

The correspondence map c (Sect. 2.2) enables accurate point-wise comparison between local features of shapes. To do this, let us consider two feature vectors $\mathbf{F}$ and $\mathbf{G}$ on meshes M_1 and M_2, respectively. Here, M_1 and M_2 belong to same individual and are measured at different time points. Our feature vector represents the geometric information of the mesh, as for instance surface point (depth) coordinates, i.e. $F(\mathbf{x}) = (x, y, z)^T$. A point-wise comparison between M_1 and M_2 can then be established from the l_2 difference of their multivariate features: $\delta(\mathbf{x}) = \|F(\mathbf{x}) - G(c(\mathbf{x}))\|^2$, at each point $\mathbf{x}$ and for a given point mapping c. This means that we could simply test the statistical significance of the difference between feature components at the corresponding vertex pairs in M_1 and M_2. However, the test statistic obtained by the simple difference would ignore the inherent correlation between deformable shapes, and consequently, would be less sensitive to small changes. Indeed, longitudinally sampled scoliotic

trunks are highly correlated when the scoliosis progresses moderately; changes in the shape deformities will therefore have very small amplitudes. One possible solution is to weight the feature vectors so that their statistical differences become significantly high. We therefore propose to combine the correspondence map with CCA [11].

Canonical Correlation Analysis (CCA) with Correspondence. The principle of CCA is to find a linear transformation that captures the relationship between two groups of multivariate vectors. Given two groups of features $\mathbf{F}$ and $\mathbf{G}$ (of n dimensions) at corresponding vertices, the canonical correlation finds, simultaneously, the weight matrices $\mathbf{a} = (a_1, ..., a_n)$ and $\mathbf{b} = (b_1, ..., b_n)$ whose column vectors are ordered w.r.t. the degree of positive correlation between $\mathbf{F}$ and $\mathbf{G}$— first canonical variates $(a_1^T\mathbf{F}, b_1^T\mathbf{G})$ are the linear combinations with the largest correlation—and the variances $\mathrm{Var}[\mathbf{a}^T\mathbf{F}]$, $\mathrm{Var}[\mathbf{b}^T\mathbf{G}]$ are equal to one. This normalization constraint ensures a uniform scaling of all the features, and therefore ensures that we get unique weight coefficients for all the corresponding points.

Our strategy is then to establish a point-wise comparison from the differences between canonical variates having maximal variance. This is analogous to finding the linear combinations with minimal (non-negative) correlation [16,17], since

$$\mathrm{Var}\{\mathbf{a}^T\mathbf{F} - \mathbf{b}^T\mathbf{G}\} = 2(1 - \mathrm{Corr}[\mathbf{a}^T\mathbf{F}, \mathbf{b}^T\mathbf{G}]). \tag{4}$$

Accordingly, differences with maximal variance are obtained by reversing the correlation order between canonical variates so that the first difference component refers to the highest variance. Point-wise comparison is consequently established between a set of canonical variates $\mathbf{a}^T\mathbf{F}$, $\mathbf{b}^T\mathbf{G}$ as follows

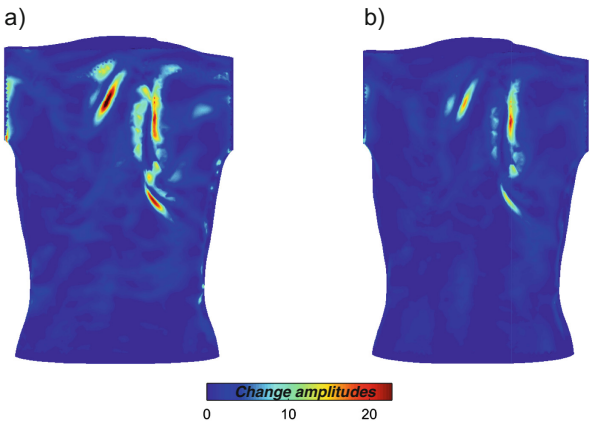

Fig. 4. Statistical change maps for a deformable scoliotic trunk shape using (a) the l_2 differences between transformed features (normal vector coordinates) with the CCA, and (b) the direct l_2 differences.

$$\delta(\mathbf{x}) = \sum_{k=1}^{m} \frac{(a_{n-k+1}^T F(\mathbf{x}) - b_{n-k+1}^T G(c(\mathbf{x})))^2}{v_{n-k+1}}, \ \mathbf{x} \in M_1 \tag{5}$$

where v_k is the $k-$th component of the variance obtained from Eq. (4). Please note that all the difference components are mutually independent. Furthermore, the linear transformation given by the CCA allows the difference components between canonical variates to approximate zero-mean normal distributions [17] at each corresponding point. Therefore, the difference measure in Eq. (5) defines the $\chi^2(m)$ test statistic with $m \leq n$ degrees of freedom. (In our application, $n = 3$, and m is set to be equal to n.) Figure 4 shows one example of how the CCA transformation can improve the power of the test statistic relative to the direct l_2 difference between matching features.

3 Results and Discussion

Our method was evaluated on 23 scoliotic patients aged 10–18 years having a right thoracic curvature in the normal spine. All the subjects were scanned at an initial visit ($t = 0$) and at 6 and 12 months from their first visit. The trunk surface meshes contained 40k to 70k vertices according to the size of the patient. The trunk model was cropped off at the arms, neck and pelvis using standard control points. These consisted of the left and right points at the corners of the acromions and of 4 anatomical landmarks located manually by an technician by palpation at the following locations: left and right anterior-superior iliac spines (ASIS), midpoint of the posterior-superior iliac spines (MPSIS) and C7 vertebral prominence (VP) [22]. The mesh boundaries were subsequently removed by interpolation (Sect. 2.1). This pre-processing step ensured that holes were filled and noise was reduced at the cropped regions. The spectral correspondence was computed by matching within-subject meshes to a template, the latter defined at the initial visit, to ensure accurate vertex-wise feature comparison across all time points. For feature comparison, we locally approximated the mesh by its tangent plane, orthogonal to the normal vector, at each point $F(\mathbf{x}) = (nx, ny, nz)^T$. We then used the CCA method to capture the differences between the local features, defined as the normal vectors, between pairs of meshes at corresponding vertices. Figure 5 shows the result of our method (spectral correspondence with CCA) for two trunk shapes at 0 and 6 months intervals for a patient who was clinically assessed with a progressive scoliosis between these successive visits. Feature vectors $\mathbf{F}$ of the first mesh (M_1) and their correspondence ($\mathbf{G}$) on the second mesh M_2 are illustrated at each vertex on M_1 for visual comparison. Significant changes in the trunk shape are indicated as the black regions on the detection map. These were identified using CCA with a $p < 0.05$ significance test.

We evaluated our method quantitatively by comparing the trunk shape changes across time to the increase of the Cobb angle (CA), a standard clinical index which measures the curvature of the spine as acquired in a radiographic image (in degrees). We therefore computed the normalized local surface area

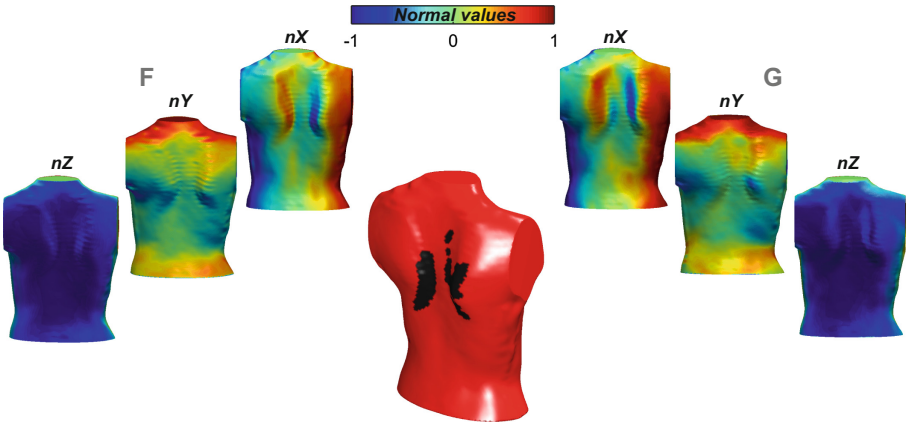

Fig. 5. Statistical analysis of local shape deformations for assessment of SP. Shown here are within-subject scoliotic trunks scanned at 0 and 6 months intervals, with a progressive thoracic spinal curve (15° increase of Cobb angle). Feature vectors **F** and **G** are represented at corresponding points on the template surface (scanned at 0 months interval). Our method reveals 3% of significant changes (in terms of the normalized local surface area) in regions located on the back (*in black on the detection map at the center*) at 5% test of significance. (Color figure online)

(in percentage) of the changes in trunk deformations during the follow-up; the local surface area of the longitudinal changes is normalized w.r.t. the total surface area of the subject's template (acquisition at $t = 0$). This normalization compensates for the different torso sizes across the population. Table 1 summarizes the CA statistics for all 23 patients as well as the averages for the progressive and non-progressive groups. For clinical purposes, a scoliosis case is considered progressive when the measured CA increases by 6° or more between 2 acquisitions. Table 2 illustrates the confusion matrix between our method and the ground truth data. This comparison shows that all 7 patients clinically evaluated as progressive had significant trunk shape changes across the two follow-up time points using our method. The average increase of the normalized area of scoliotic deformities was $(2.7 \pm 1.8)\%$, whereas the average increase in CA across this group was 9°. This means that for this group of patients, whose spinal deviations progressed moderately, the proposed method was able to capture, on average, 2.7% change in the shape deformations associated with SP. Moreover, significant shape changes were detected in 4 out of 16 non-progressive scoliotic patients. These cases are reported as false positives with respect to the ground truth clinical assessment. They are mainly due to outliers located at the cropped boundaries of the trunk. The uncertainty in the placement of the anatomic landmarks leads to variability in the cropping of the trunk model and therefore to uncertainty errors in matching the boundary regions. On the other hand, SP is evaluated clinically solely on the basis of deviations of the spine through CA measurement. But the CA remains limited to assessing the spinal deformity in a 2D radiographic projection, while the shape of the scoliotic trunk is also affected

Table 1. Summary CA statistics for 23 scoliotic trunks characterized by a right thoracic spinal curve (in degrees).

t (mo)	Max	Mean	SD	Mean of progressive group	Mean of non-progressive group
0	47	21	18	37	15
6	58	28	20	46	22
12	59	29	21	51	22

Table 2. Confusion matrix for categorization of patients as progressive or non-progressive: our method versus standard clinical method based on CA.

		Ground truth measurements (CA)	
		Progressive	Non-progressive
Proposed method	Change	7	4
	No change	0	12
Total		7	16

by other factors, in particular the deformation of the rib cage (manifested as a hump at the back). This latter deformation is caused by the axial rotation of vertebrae [10]. Figure 6 shows one case of a follow-up patient whose scoliosis was considered non-progressive according to the CA, while a hump at the back progressed significantly between the 6 and 12 month time points. This is considered as a false positive according to the CA assessment. Rib hump deformation is in fact one of the first diagnostic indicators of scoliosis, in particular during its early stages; it is also one of the most visible signs affecting the cosmetic appearance of the trunk, which is the major concern of young patients [5,23]. Our preliminary results demonstrate the importance and the effectiveness of including longitudinal shape analysis in scoliosis assessment routines. We aim to strengthen these results by means of larger datasets and more extensive validation. Moreover, in order to efficiently evaluate SP, we excluded in this work all possible changes on the anterior side of the trunk. These changes, particularly observed in young female patients, are affected by the deformation of the chest, which might be due to different factors: asymmetry changes associated with scoliosis, position of the arms or growth; they might therefore lead to ambiguity in SP assessment. Even with a standardized positioning of the arms, the morphological correlation between the normal anatomical changes of the body (e.g., body fat and growth) and scoliosis deformations prompted us to focus on the posterior side of the trunk. Analysis of full-torso changes would require an evaluation of the normal variability of scoliotic trunk shapes during the anatomical development of adolescents.

Finally, we evaluated the performance of the point-wise statistical analysis using the CCA transformation of shape features against direct comparison, i.e., simple point-wise differences (Sect. 2.3). For this evaluation, we compared the increase in the normalized local surface area of the trunk deformations during

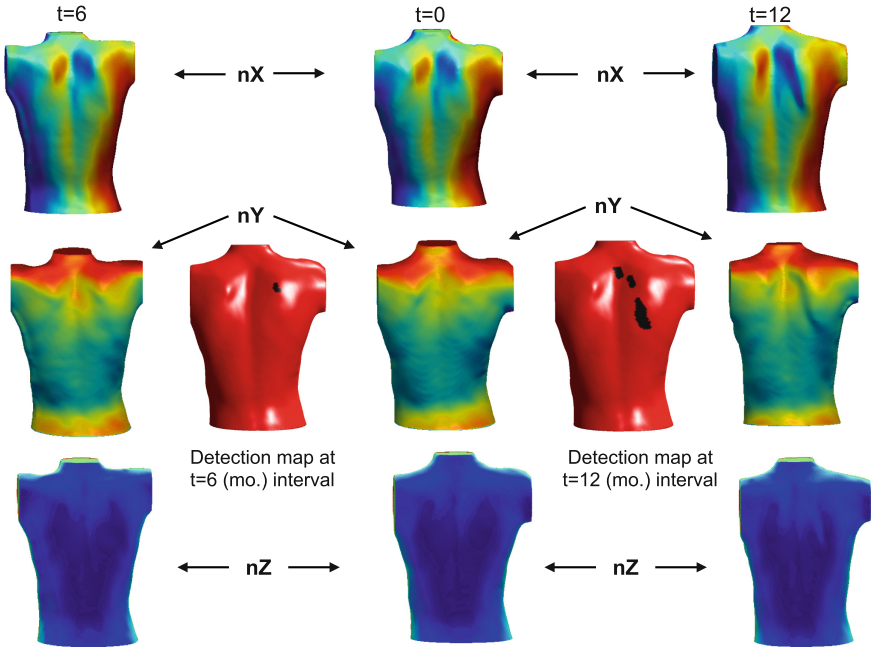

Fig. 6. One progressive case considered as a false positive compared to the CA ground truth. Middle column: feature vector (normal vector coordinates $\mathbf{F}(\mathbf{x}) = (nx, ny, nz)$) of the scoliotic trunk at the initial visit ($t = 0$ mo. interval). Left and right columns: shape features at $t = 6$ and $t = 12$ mo. intervals, respectively. Detection maps are obtained using spectral correspondence to $t = 0$ and CCA for 5% test of significance.

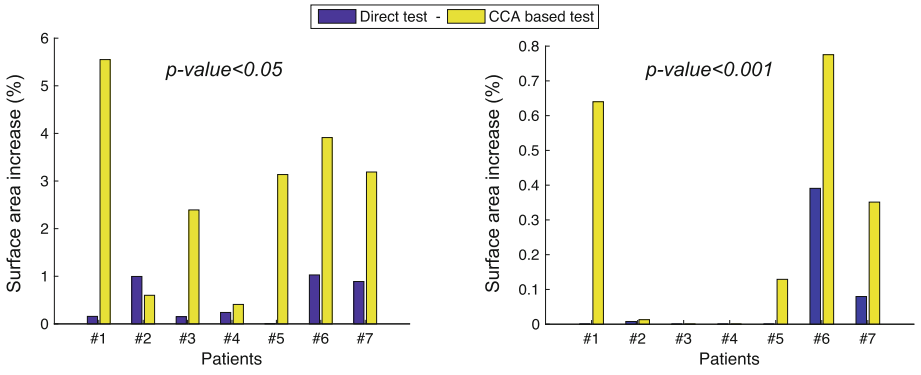

Fig. 7. Performance of the statistical analysis using CCA transformation of matching features versus direct comparison, for the follow-up of 7 progressive cases. The CCA significantly improves the test statistic for both $p < 0.05$ and $p < 0.001$.

the follow-up of the 7 patients having progressive scoliosis. Figure 7 shows that the CCA significantly improves the detection power of the χ^2 test statistic (for $p < 0.05$ and $p < 0.001$). On average, a 2.74% increase in the surface area is detected by the CCA method for $p < 0.05$, and 3.22% for $p < 0.001$, while the test using direct comparison detects only very small areas of change in the shape deformities (0.5% for $p < 0.05$ and 0.08% for $p < 0.001$). Further research could investigate whether a statistical model [2] that considers the spatial relationship between each vertex and its neighborhood can improve the underlying point-wise statistical analysis.

4 Conclusion

In this contribution, we addressed longitudinal shape analysis of scoliotic trunks using a spectral representation of surface models and point-wise feature comparison via CCA. The main originality of our work is the spectral representation and the efficient computation of shape correspondences in order to compare different scoliotic trunks over time. For the first time, scoliotic trunk analysis is based on the spectral representation of shapes. However, correct shape correspondence remains a challenging problem in our context because of the variability between acquisitions in the cropping of the surface models at the trunk boundaries. Future work will focus on this issue. In our validation study, we considered a single type of scoliotic deformation to test the performance of our method against the standard evaluation based on Cobb angles. Quantitive comparison with the clinical ground truth demonstrates the effectiveness of our shape analysis method for scoliosis follow-up and progression assessment.

Future work will be threefold: we will focus on the issue of shape matching in the presence of uncertainty at the trunk boundaries; we will consider larger patient sets including several scoliotic deformation types for validation; finally, we will look at adapting this framework for other applications such as predicting scoliosis progression and evaluating the effect of spine correction on trunk asymmetry.

Acknowledgments. This research was funded by the Canadian Institutes of Health Research (grant number MPO 125875). The authors would like to thank Philippe Debanné for revising this paper and the anonymous reviewers for their insightful comments and suggestions.

References

1. Adankon, M.M., Chihab, N., Dansereau, J., Labelle, H., Cheriet, F.: Scoliosis follow-up using noninvasive trunk surface acquisition. IEEE Trans. Biomed. Eng. **60**(8), 2262–2270 (2013)
2. Ahmad, O., Collet, C.: Scale-space spatio-temporal random fields: application to the detection of growing microbial patterns from surface roughness. Pattern Recogn. **58**, 27–38 (2016)

3. Ajemba, P.O., Durdle, N.G., Raso, V.J.: Characterizing torso shape deformity in scoliosis using structured splines models. IEEE Trans. Biomed. Eng. **56**(6), 1652–1662 (2009)
4. Belkin, M., Niyogi, P.: Laplacian eigenmaps for dimensionality reduction and data representation. Neural Comput. **15**(6), 1373–1396 (2003)
5. Buchanan, R., Birch, J.G., Morton, A.A., Browne, R.H.: Do you see what I see? Looking at scoliosis surgical outcomes through orthopedists' eyes. Spine **28**(24), 2700–2704 (2003). discussion 2705
6. Carr, J.C., Beatson, R.K., Cherrie, J.B., Mitchell, T.J., Fright, W.R., McCallum, B.C., Evans, T.R.: Reconstruction and representation of 3D objects with radial basis functions. In: Proceedings of the 28th Annual Conference on Computer Graphics and Interactive Techniques, SIGGRAPH 2001, pp. 67–76. ACM, New York (2001)
7. Cobb, J.R.: Outline for the study of scoliosis. Am. Acad. Orthop. Surg. Instruct. Lect. **5**, 261–275 (1984)
8. Fischl, B., Sereno, M.I., Tootell, R.B., Dale, A.M.: High-resolution intersubject averaging and a coordinate system for the cortical surface. Hum. Brain Mapp. **8**(4), 272–284 (1999)
9. Grigis, A., Noblet, V., Heitz, F., Blanc, F., de Sèze, J., Kremer, S., Rumbach, L., Armspach, J.P.: Longitudinal change detection in diffusion MRI using multivariate statistical testing on tensors. NeuroImage **60**(4), 2206–2221 (2012)
10. Hackenberg, L., Hierholzer, E., Pötzl, W., Götze, C., Liljenqvist, U.: Rasterstereographic back shape analysis in idiopathic scoliosis after posterior correction and fusion. Clin. Biomech. **18**(10), 883–889 (2003)
11. Hotelling, H.: Relations between two sets of variates. Biometrika **XXVIII**, 321–377 (1936)
12. Jain, V., Zhang, H.: Robust 3D shape correspondence in the spectral domain. In: IEEE International Conference on Shape Modeling and Applications 2006 (SMI 2006), p. 19, June 2006
13. Lombaert, H., Grady, L., Polimeni, J.R., Cheriet, F.: FOCUSR: feature oriented correspondence using spectral regularization-a method for precise surface matching. IEEE Trans. Pattern Anal. Mach. Intell. **35**(9), 2143–2160 (2013)
14. Lombaert, H., Arcaro, M., Ayache, N.: Brain transfer: spectral analysis of cortical surfaces and functional maps. Inf. Process. Med. Imaging **24**, 474–487 (2015)
15. Lombaert, H., Grady, L., Pennec, X., Ayache, N., Cheriet, F.: Spectral demons-image registration via global spectral correspondence. In: Fitzgibbon, A., Lazebnik, S., Perona, P., Sato, Y., Schmid, C. (eds.) Computer Vision - ECCV 2012. LNCS, vol. 7573, pp. 30–44. Springer, Heidelberg (2012)
16. Nielsen, A.: The regularized iteratively reweighted MAD method for change detection in multi- and hyperspectral data. IEEE Trans. Image Process. **16**(2), 463–478 (2007)
17. Nielsen, A.A., Conradsen, K., Simpson, J.J.: Multivariate alteration detection (MAD) and MAF postprocessing in multispectral, bitemporal image data: new approaches to change detection studies. remote Sens. Environ. **64**(1), 1–19 (1998)
18. Pazos, V., Cheriet, F., Danserau, J., Ronsky, J., Zernicke, R.F., Labelle, H.: Reliability of trunk shape measurements based on 3-D surface reconstructions. Eur. Spine J. **16**(11), 1882–1891 (2007)
19. Reuter, M.: Hierarchical shape segmentation and registration via topological features of laplace-Beltrami eigenfunctions. Int. J. Comput. Vis. **89**(2–3), 287–308 (2009)

20. Reuter, M., Wolter, F.E., Peinecke, N.: Laplace-spectra as fingerprints for shape matching. In: Proceedings of the 2005 ACM Symposium on Solid and Physical Modeling, SPM 2005, pp. 101–106. ACM, New York (2005)
21. Richards, B.S., Bernstein, R.M., D'Amato, C.R., Thompson, G.H.: Standardization of criteria for adolescent idiopathic scoliosis brace studies: SRS committee on bracing and nonoperative management. Spine **30**(18), 2068–2075 (2005). Discussion 2076–2077
22. Seoud, L., Dansereau, J., Labelle, H., Cheriet, F.: Multilevel analysis of trunk surface measurements for noninvasive assessment of scoliosis deformities. Spine **37**(17), E1045–E1053 (2012)
23. Tones, M., Moss, N., Polly, D.W.: A review of quality of life and psychosocial issues in scoliosis. Spine **31**(26), 3027–3038 (2006)